MINERAL ALTERATION IN ACID AND NEUTRAL-pH HYDROTHERMAL RESERVOIR : THE CASE OF MAHANAGDONG GEOTHERMAL FIELD, LEYTE

Ma. Victoria M. Martinez

Geoscientific Department, PNOC-Energy Development Corporation,
Fort Bonifacio, Makati City, Philippines

Abstract

The silicate and sulfide mineral equilibria for the Mahanagdong Geothermal Field production wells were investigated using mineral activity diagrams. Evaluation of silicates focused on K-, Na- and Ca-bearing minerals which are the most widely distributed alteration minerals in the reservoir. The stability of these minerals depends on three factors, namely, temperature, concentration of the cation species, and pH of the fluids. Among the silicate minerals, the following are in equilibrium with the Mahanagdong jluids: K-mica (illite), wairakite, kaolinite, epidote and K-feldspar. Geologic logging of the cuttings has confirmed the presence of these minerals in the open hole section of both neutral and acid wells in Mahanagdong. It is evident, therefore, that no silicate minerals can be used to distinguish the acid from the neutral-pH fluids in this field.

The stability or activity of the sulfide minerals are governed by two factors. These are the pH and the redox state (expressed in terms of O_2 fugacity) of the fluids. Surfide minerals in equilibrium with both neutral and acid fluids are pyrite, chalcopyrite and bornite. Among the dissolved species of sulfur, H_2S is likewise in equilibrium with both fluid types. Together these indicate that the fluids in Mahanagdong have already evolved from a magmatic to a hydrothermal system.

Aside from silicate and sulfide mineral equilibria, calcite and anhydrite saturation for each Mahanagdong well were also evaluated. Wells which showed anhydrite supersaturation are the acid wells situated in the northern part of the field. This condition is attributed to their inherent high SO_4 concentration. Wells which exhibited calcite saturation and supersaturation at reservoir condition are the neutral-pH wells in the outflow zone of the sector.

1.0 Introduction

The Mahanagdong sector is located in the southeasternmost portion of the Greater Tongonan Geothermal Field in northwestern Leyte (Fig. 1). The field is programmed for large-scale power generation which is to be interconnected to the Leyte-Luzon grid. Testing of the wells dnlled in the area has identified two types of fluids residing in the reservoir : acid and neutral-pH. The wells drilled in the central and southern regions tapped the neutral-pH reservoir while the northern sector wells drilled into the acid reservoir. These fluids, however, can be further characterized into the following types: neutral-pH fluids with high gas content; neutral-pH fluids with low-gas content; cooler neutral-pH fluids; and acid fluids with low-gas content. From these, three areas have been delineated and considered as constraints during the development phase of the sector. These are the high-gas zone in the eastern side of the field, the acid zone in the north and the area of colder fluids in the west (Fig. 2).

This paper was developed to evaluate the equilibria of secondary hydrothermal minerals with these different types of fluids. The primary aim of this study is to relate the chemistry of the fluids with the stable mineral phases in the wells. Its most important implication is the determination of the secondary mineral assemblages formed under the different types of fluids percolating in the area. Corollary to this is the assessment of the potential of the fluids to effect deposition of vein minerals.

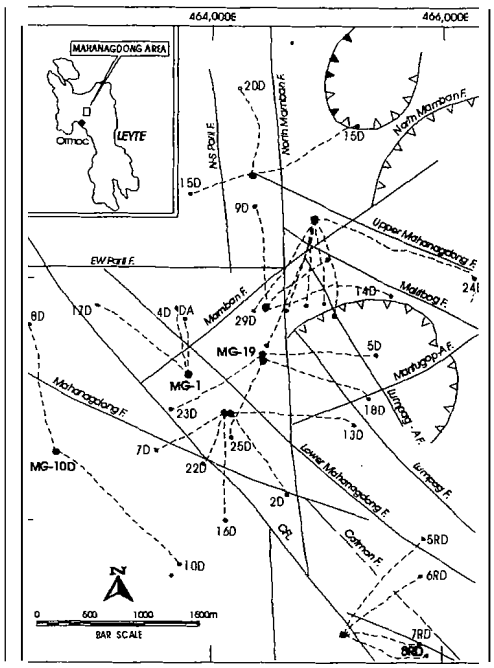

Fig. 1 : ***Location map of Mahanagdong Geothermal Field***

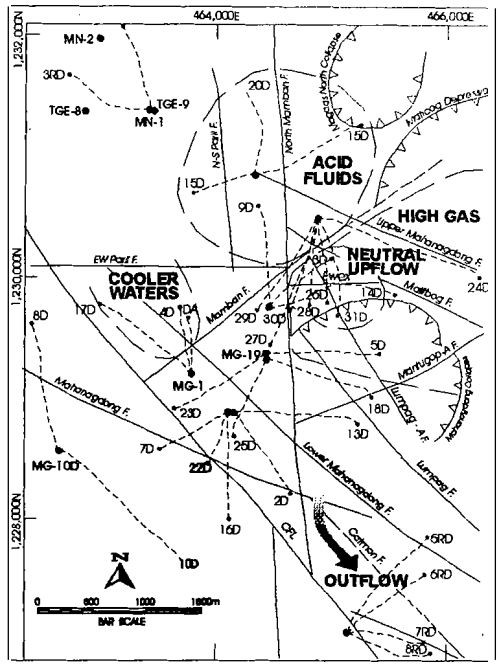

Fig. 2 : ***Hydrogeochemical model of Mahanagdong Geothermal Field showing the different chemical constraints (after Parrilla, et.al, 1995; Zaide-Delfin,et.al, 1996***

2.0 Methodology

The most important and widely used tool in the evaluation of mineral equilibria is the stability or activity dagram. Utilization of this diagram permits evaluation of whether the fluids are in equilibrium with certain minerals at reservoir conditions. In low-pH fluid reservoir or lughly oxidizing environment, the minerals are unstable and tend to be dissolved. Otherwise, the minerals will remain fixed in the rock or they tend to precipitate from the solution (Arnorsson, 1992).

Stability diagrams are the graphical representations of the activity of minerals at different reservoir condtions. The first step in the construction of these diagrams is to decide what minerals to relate with the fluid chemistry. This is usually done by choosing the most abundant and common secondary hydrothermal minerals observed in drill cuttings/core. In all geothermal fields in the Philippines includmg Mahanagdong, the reservoir rocks are extensively altered by silicate and sulfide minerals (*Dulce,* et al., 1995). Thus, these minerals were selected for the evaluation.

The construction of mineral diagrams involves the use of thermochemical data, equilibrium constants, field data, and experimental data. Thermochemical data (i.e. Gibbs free energy of formation of minerals) are used to calculate for the activities of the minerals. The minerals' Gibbs free energy of formation as calculated by Helgeson, et al. (Arnorsson, 1992) were utilized for this evaluation.

The deep fluid composition for each well was determined using the WATCH speciation software of Arnorrson (1990). The reservoir temperature for each well were taken from their quartz geothermometer and when available and applicable from the measured temperatures. Representative water and gas discharge chemistry are listed in Tables 1 and 2, respectively.

3.0 Silicate Mineral Equilibria

In Mahanagdong, the most common types of silicates are K-mica, K-feldspar, wairakite, albite, epidote, and kaolinite. The stability of these minerals are governed by the concentration of the major cations (K, Ca, Na, Mg), the temperature and pH of the fluids reacting with the host rocks. In the stability diagrams, the transition or boundaries between the silicate minerals represent the activities of the cations participating in the reaction at different temperatures.

A stability dlagram was constructed for each dominant cation species (K-beanng, Na-bearing and Ca-bearing silicates). After the stability diagrams were constructed, the speciated components of the fluids were then plotted in the diagrams. The succeeding sections discuss the results of the plot.

3.1 $K_2O - SiO_2 - H_2O - Al_2O_3$ system

The plot of the Mahanagdong wells in the K-stability dlagram is shown in Figure 3. All of the wells, except for MG-4D, plot inside the K-mica stability field. This implies that the wells are in equilibrium with the mineral K-mica. Based on petrological data, all of the wells have been observed to contain K-mica. It is evident from the plot, though, that the acid wells (MG-20D, MG-21D, MG-15D, MG-9D) are approaching the k-mica-kaolinite boundary, nearer to the acid mineral kaolinite.

MG-4D has tapped fluids with low temperature (190 °C) probably as a result of mixing of the original deep brine with cooler inflows (i.e. shallow recharge condensate). The low-temperature fluid of the well when plotted in the stability diagram plots on the kaolinite field. This does not mean that the waters of MG-4D is acid as discharged waters yield neutral-pH. This only implies that the K-stability diagram is not applicable with the fluids of MG-4D since K-bearing clays are formed at a temperature of ≥220°C. Similarly, in the Na- and Ca- bearing silicate stability diagrams, MG-4D plotted on the kaolinite field, again implying that these diagrams are not applicable to the fluids of MG-4D.

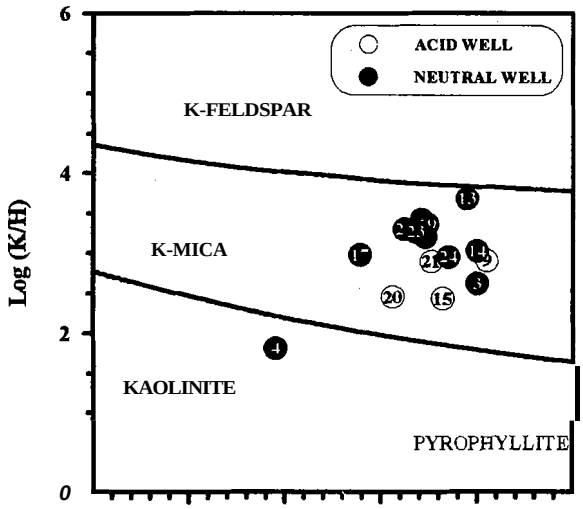

The clustering of both acid and neutral-pH wells inside the K-mica stability field implies that both fluid types have attained equilibrium with the mineral. Potash-mica have been thought before as a neutral-silicate; however, its occurrence in the acid wells in Mahanagdong implies fhat it can also be stable under acid conditions.

3.2 $Na_2O - SiO_2 - H_2O - Al_2O_3$ system

Figure 4 represents the plot of the wells in the Na-bearing silicate stability diagram. Wells MG-3D, 9D, 20D, 15D, 21D, 24D, and 14D all plotted in the kaolinite field Again, this does not mean that MG-24D, 14D and 3D are acid wells. This just implies that Naclays are less favored to be formed by the fluids or waters of these wells. Instead, K-clays are most likely to be formed as what has been observed in the K-bearing diagram. On the other hand, low albite will be formed from the fluids of MG-7D, 23D, 19, 18D, 16D and 13D.

The plot tells us that the acid fluids and neutral-pH fluids are both in equilibrium with the Na-bearing silicate mineral in the reservoir. This suggests equilibration of the acid fluids with the surrounding rocks.

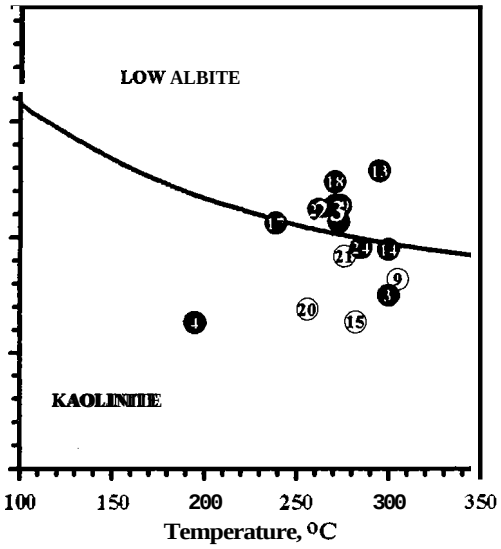

Fig. 4 : ***Stability diagram for Na-bearing silicates***

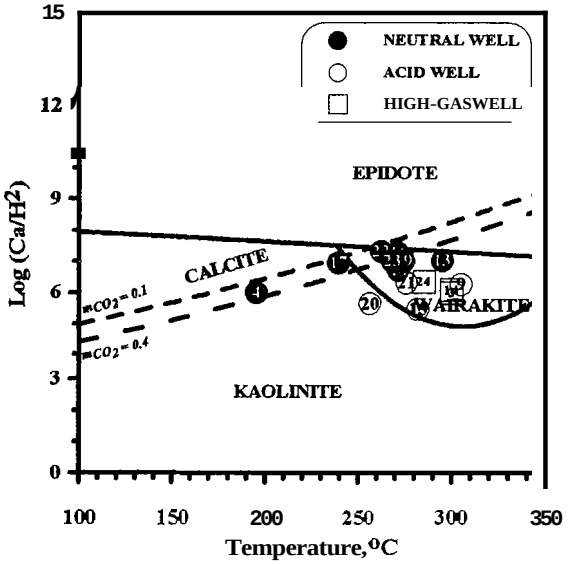

Fig. 5 : ***Stability diagram for Ca-bearing silicates***

3.3 $CaO - SiO_2 - H_2O - Al_2O_3 - CO_2$ system

The plot of the wells in the calcium stability dagram (Fig. *5)* likewise shows the stability of both the acid and neutral wells with wairalate and epidote. For calcium-bearing silicates, the amount or content of CO_2 in the fluid is considered in the reaction as this has a great effect on the formation of minerals. In the presence of high amount of CO_2, calcite mineral is more likely to be formed instead of epidote. The concentration range of CO_2 in Mahanagdong wells are plotted in the dlagram, representing the calcite blind. As the CO_2 content increases the calcite field increases while epidote field disappears.

The high gas wells, MG-3D, MG-9D and MG-14D, are in equilibrium with wairakite. However, from the plot we *can* deduce that at lower reservoir temperatures (~220°C), their fluids could favor the formation of calcite. At their present reservoir temperatures, the wells' proximity to the wairakite-calcite-epidote boundary imply that these minerals *can* possibly coexist.

4.0 Sulfide Mineral Equilibria

The most common sulfides and oxides observed in the Mahanagdong cuttings are pynte (FeS_2), chalcopynte ($CuFeS_2$), bornite ($CuFeS_4$), hematite (Fe_2O_3) and magnetite (Fe_3O_4). The stability of sulfides at different reservoir temperature are shown in Figures 6-11. The solubilities of these minerals are controlled by the fluid pH, the redox state of the fluids and temperature. *As* temperature decreases, hematite field increases while that of pyrrhotite decreases. Pyrrhotite are formed under a high temperature and reducing environment whereas hematite tends to form at low temperature and oxidizing environment.

Activity diagrams were constructed each for 200°C, 240°C, 260°C, 270°C, 280°C and 300°C reservoir temperature. The 300-degree regime includes wells MG-3D, MG-14D, MG-13D and MG-9D. These wells are interpreted to be tapping the parent fluids of the sector since they have the highest temperature. The other temperatures represent the different outflow temperatures of the fluids. Wells MG-24D, MG-21D and MG-15D are grouped into the 280-degree temperature regime. Five wells are included in the 270-degree plot (MG-7D, MG-16D, MG-18D, MG-19 and MG-23D). For the 260-degree plot, wells MG-20D and MG-22D are grouped together. The low temperature wells, depicted by MG-4D and MG-17D are placed in the 200- and 240-degree regimes, respectively.

Wells MG-3D, MG-9D, MG-13D and MG-14D (Fig.6) all plot within the pyrite and chalcopyrite stability field. This means that for these wells, pyrite and chalcopyrite are the dominant stable sulfide phases. The same is true for wells in the 280-degree plot (Fig.7). Wells MG-15D, MG-21D and MG-24D are in equilibrium with pyrite and chalcopyrite.

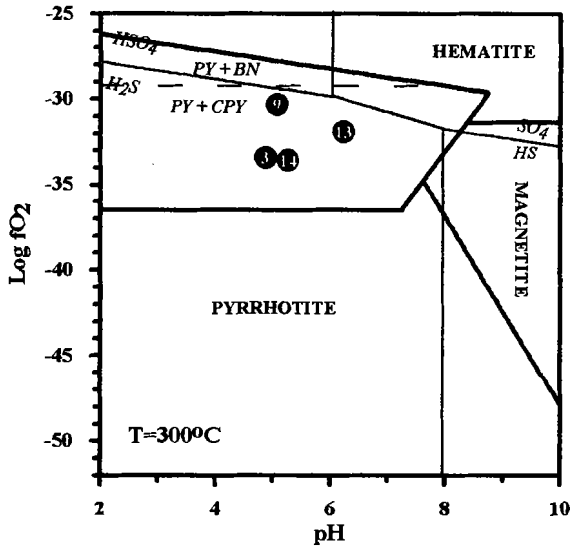

Fig. 6 : *Sulfide stability diagram for 300°C*

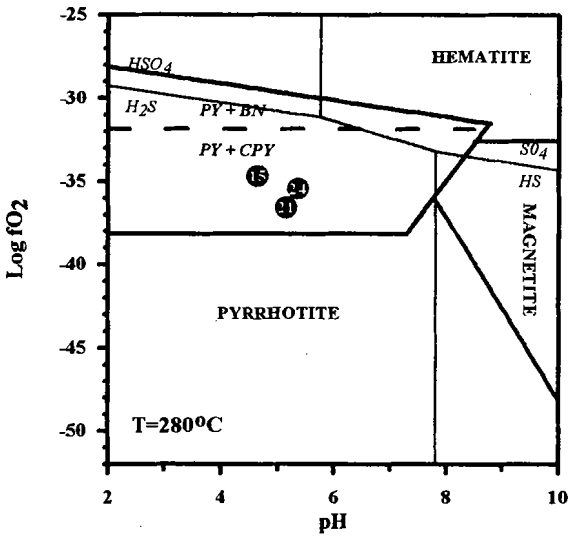

Fig. 7 : *Sulfide stability diagram for 280°C*

For wells belonging to the 270-degree regime (Fig. 8), MG-18D, MG-16D and MG-19 plot close to the chalcopyritye-bornite boundary. Their proximity to the boundary implies that aside from chalcopyrite, the mineral bornite could be a stable phase for these wells. This statement is supported by petrologic data as bornite is present in the wellbores.

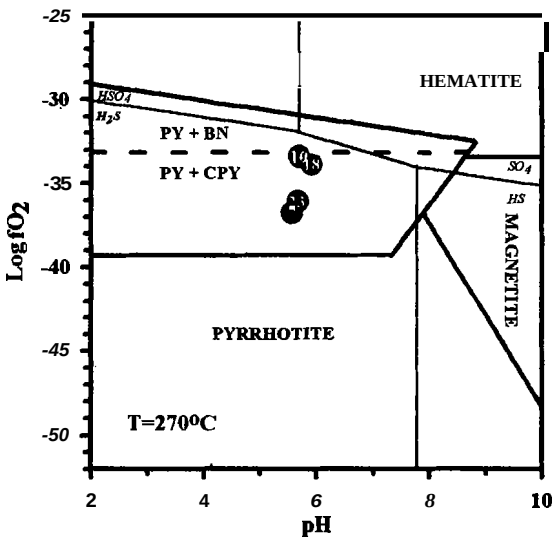

Fig. 8 : *Sulfide stability diagram for 270°C*

Wells MG-20D and MG-22D (Fig. 9) plot inside the pynte and chalcopynte stability field. MG-17D (Fig. 10) plotted on the pynte and bornite field, whle MG-4D (Fig. 11) plotted on the pynte and chalcopyrite field.

The dominant sulfur species for all the wells is H_2S. This implies that the Mahanagdong sector has already evolved from a magmatic system dominated by the sulfur species SO_4 and SO_2 into a hydrothermal system with H_2S as the dominant sulfur species.

The similarity of stable sulfide minerals under the acid and neutral-pH reservoir based on stability diagrams, implies that at reservoir condition both fluid types produce similar sulfide mineralogy. A study conducted by Dulce, et al (1995) on the sulfide mineralogy of Mahanagdong, however, has revealed that acid fluids produce more sulfides in comparison with the neutral fluids. Although both fluids are stable with the same mineral, there is an abundance of sulfides in acid wells than in neutral wells.

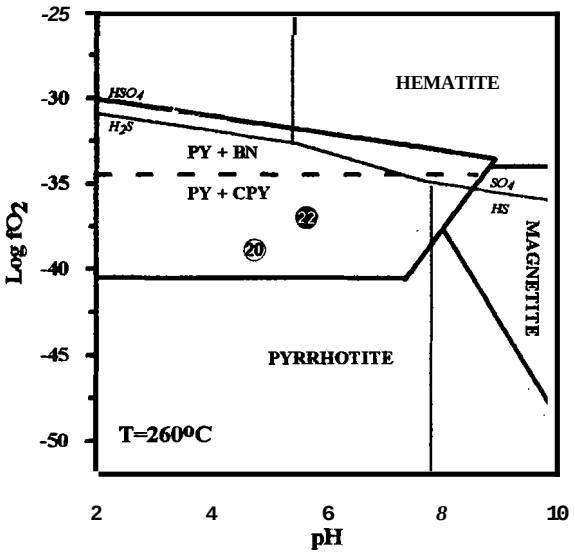

Fig. 9: *Sulfide stability diagram for 260°C*

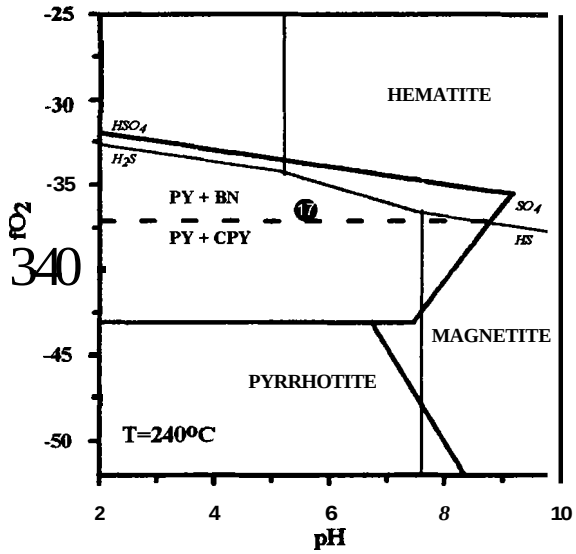

Fig. 10 : *Sulfide stability diagram for 240°C*

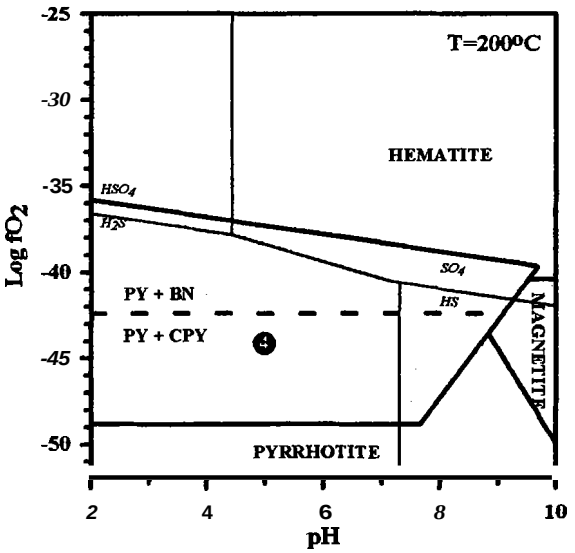

Fig. 11 : *Sulfide stability diagram for 200°C*

5.0 Calcite and Anhydrite Saturation

Aside from the evaluation of the equilibria between the fluids and the minerals, the potential of calcite and anhydrite to precipitate was also assessed. The WATCH speciation software was utilized for the calculation of the solubilities of these minerals in all of the wells.

Figures 12 and 13 represent the saturation of the fluids with calcite and anhydrite, respectively. The calculated solubilities of the minerals for each well were plotted against the fluids' reservoir temperature. The equilibrium line (diagonal line in the graph) represents the theoretical mineral solubilities at corresponding reservoir temperatures. Points that plot above the line denote supersaturation with the mineral, hence the potential to form veins. On the other hand, plotting below suggests unsaturation with the mineral.

The neutral-pH fluids appear to be supersaturated with calcite and thus the potential to form veins. The acid fluids, on the other hand plotted below the line, indicating the preference of calcite to be dissolved under acidic environment. (Salonga, 1995).

The opposite trend is observed for the anhydrite saturation diagram. The acid fluids plot above the line implying their supersaturation with the mineral, while the neutral-pH fluids are unsaturated with anhydrite. Aside from the acid fluids, some wells which have tapped neutral-pH fluids also show saturation and oversaturation with the mineral. This could be attributed to the relatively high SO_4 content of these wells similar to the acid fluids.

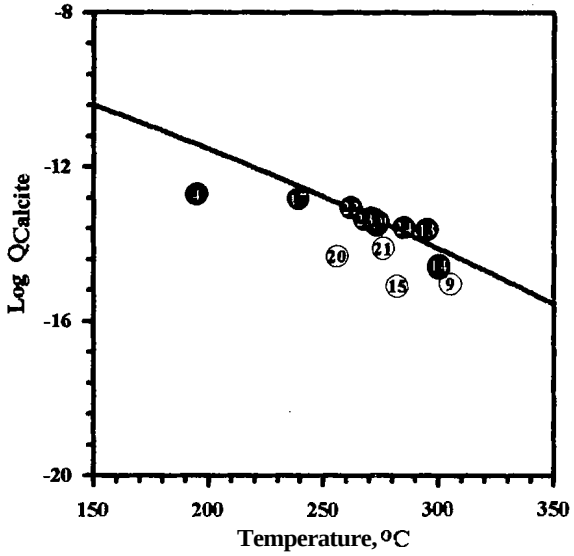

Fig. 12: *Saturation diagram for calcite*

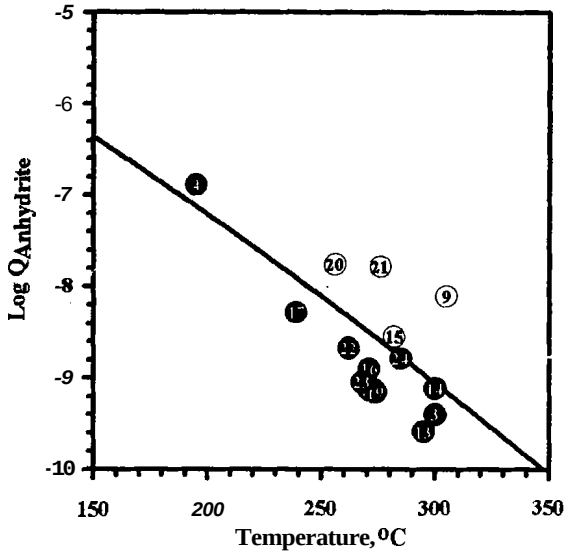

Fig. 13: *Saturation diagram for anhydrite*

6.0 Discussion

Based on the plots of the fluids with respect to the activity of the mineral phases at reservoir condition, no distinct differences are observed between acid and neutral-pH fluids. Both types of fluids plot on the same mineral stability field and are therefore stable with similar silicate and sulfide minerals. These findings are supported by actual petrological data and are consistent with postulated hydrothermal system.

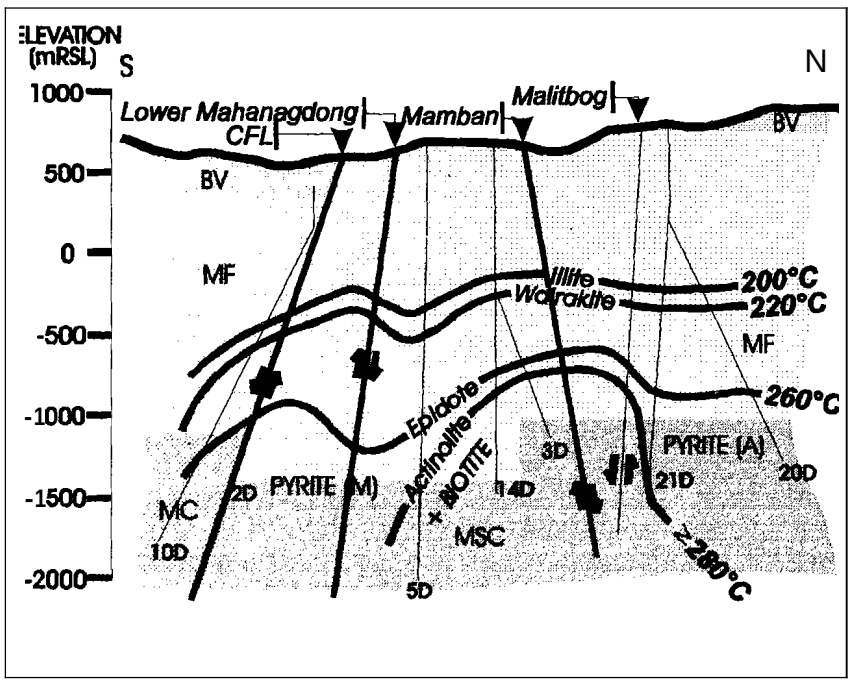

Fig. 14: *Cross-section of Mahanagdong Geothermal Field. Shown are the first appearances of minerals with corresponding subsurface temperatures*

The hottest sector of the field is tapped by wells MG-3D, MG-14D and MG-9D (Fig. 14). These wells delineate the upflow zone of the system. Wells MG-3D and MG-14D both discharged neutral fluids while MG-9D discharged acid fluids. Fluids tapped in the upflow zone have the following stable mineral phases: illite (k-mica), albite, wairakite, epidote, pyrite, bornite and chalcopyrite. This region corresponds to the inner propylitic zone of Meyer and Hemley (Hedenquist, 1987). The inner propylitic zone is characterized by the presence of epidote and actinolite as the key minerals with illite and chlorite as accessory minerals. These minerals indicate passage of hot (300°C) neutral-pH fluids with relatively high Ca^{++} content. This is consistent with the chemistry of the fluids discharged by the wells drilled in this area.

Wells drilled on the southern sector discharged neutral-pH fluids with temperatures of 250-270°C. The fluids produced albite, illite, wairalate, epidote, pyrite and chalcopynte ass hydrothermal alterations. Basing on the alteration assemblage model of Meyer and Hemley (1987), these wells were dnlled within the propylitic zone. These zones are characterized by the presence of epidote as the key mineral with illite and sulfides as accessory minerals. Moreover, the chemistry of the altering fluids are of neutral-pH with significant amounts of Ca^{++} and K^{+} and a temperature of $\geq$250°C. This area defines the neutral outflow of the system.

The presence of the cold recharge in the western part of the field was detected through wells MG-4D and MG-17D. MG-4D has a temperature of around 190°C, wlule MG-17D has a temperature of about 235°C (Parrilla, et. al., 1995). The constructed stability diagrams cannot be applied for MG-4D mainly because of the low temperature of the fluid. The silicate minerals included in the diagrams have formation temperatures of at least 220°C; thus the fluids of MG-4D are not in equilibrium or compatible with these minerals. However, based on petrological' data, MG-4D has been observed to contain some high temperature minerals, like wairakite and epidote. This indicates that MG-4D has fluids originally of high temperature (around 270°C). However, recent occurrences of cold water inflow effected a low temperature for the well during its discharge (Zaide-Delfin, et.al., 1996).

MG-17D, on the other hand, still has a relatively higher temperature compared to MG-4D. However, its temperature of 235°C does not represent the true temperature of the fluids percolating in the area. Just like in MG-4D, high temperature minerals have also been observed in this well. Thus, the low temperature measured for the well represents that of the mixed fluid. The relict alteration assemblages of MG-4D and MG-17D would still fall under the propylitic zone of Meyer and Hemley.

The acid wells, MG-15D, MG-20D, and MG-21D are distinctively separated from the neutral wells and they are also interpreted as outflow in the north. However, the fluids are acidic in nature. The stable mineral phases are similar to the neutral-pH wells. The main reason for the similarity of the mineral assemblages between the neutral-pH and the acid fluids is their similar pH at reservoir condition (4-5). Moreover, both acid and neutral fluids could have already attained some degree of equilibrium with the host rocks. Under Meyer and Hemley's model, these wells would be classified under the transition zone from advanced argillic to propylitic zone. Minerals under the advanced argillic zone such as pyrophyllite, diaspore and andalusite are effected by an acid pH fluid. Some of the acid wells have been observed to contain pyrophyllite. However, most of the alteration assemblages are characteristic of the propylitic alteration zone. MG-9D, wluch is grouped into the wells which may have tapped the parent fluids, is also classified under this zonation because of the acidic nature of its fluids.

Evaluation for anhydnte and calcite saturation have shown that the acid wells are supersaturated with the mineral anhydnte at reservoir condition, thus the tendency to form veins. Tlus is attributed to the relatively high sulfate content of these fluids compared to the neutral-pH fluids at reservoir condition. Aside from the acid wells, one neutral-pH well have also shown supersaturation with anhydrite. This is also due to the hgh sulfate content of the fluid of this well which is interpreted to be caused by the dilution of a colder, high-sulfate fluid. The neutral-pH fluids, on the other hand, have the preference to form calcite veins instead of anhydrite. The acid wells' unsaturation with calcite implies the preference of the calcite to be dissolved at lower pH (Salonga, 1995).

7.0 Conclusions

Acid and neutral-pH fluids are both present in the geothermal reservoir of Mahanagdong. These fluids are stable with the Same silicate minerals k-mica (illite), epidote, wairakite, kaolinite and k-feldspar. Similarly, both fluid types are stable with the sulfide minerals pyrite, chalcopyrite and bornite.

The similarity of the stable mineral phases for both fluid types implies that there are no distinct silicate and sulfide mineral assemblages to distinguish acid from the neutral-pH fluids. Among the dissolved sulfur species, H_2S is in equilibrium with both acid and neutral-pH fluids. These indicate that the fluids have already evolved from a magmatic to a hydrothermal system.

With regards to the potential of the fluids to effect vein formation, the acid fluids along with MG-4D yielded positive for anhdyrite deposition, which is basically attributed to their high sulfate content. Calciting, on the other hand, is positive for the neutral wells.

References

Arnorrson, S., 1990. WATCH 2.1 - A speciation software.

Amorsson, S., 1992. A Summary of Basic Thermodynamic Relations and the Methodology of Calculating the Thermodynamic Processes of Minerals at Different Temperature and Pressure. Lecture notes.

Auman. R., 1995. The Geochemistry of the First Medium-Term Discharge of Well MG-14D. PNOC-EDC Internal Report.

Dulce, R.G., J.B. Rosell, and M.C. Zaide-Delfin, 1995. Sulfide Minerals as Indicators of Acid Cl-SO_4 Fluids. Proceedings of the 1996 PNOC-EDC Geothermal Conference, 137-149 pp.

Hedenquist, J.W., 1987. A short course discussing the important aspects of epithermal mineralization. Lecture notes.

Henley, R.W., A.H. Truesdell and P.B.Barton, Jr., 1984. Fluid-Mineral in Hydrothermal Systems, Vol.1. Bookcrafters, Inc, MI., 268 pp.

Parrilla, E.V., O.T.Jordan, J.R.Ruaya, 1995. Geochemistry Resource Assessment Update, Mahanagdong Geothernial Field, Leyte Geothermal Power Project. PNOC-EDC Internal Report.

Reyes, A. G., 1990. Petrology of Philippine Geothermal Systems and the Application of Alteration Mineralogy to their Assessment. Journal of Volcanology and Geothermal Research, 43, pp. 279-309.

Salonga, N.D., 1995. Fluid- Mineral Equilibria in Acid NaCl(+SO4) Reservoir : The Case of Sandawa Collapse, Mt.Apo Hydrothermal System. PNOC-EDC Internal Report.

TML, 1983, Fluid-Mineral Equilibria. PNOC-EDC In-house training manual.

Zaide-Delfin, M.C. and R.G.Dulce. '1996. Hydrothermal Petrology and Fluid Flows in the Mahanagdong Geothermal Field, Leyte, Phlippines. PNOC-EDC Internal Report.

Table 1 : Representative Water Discharge Chemistry

Well Name	Date	Source	WHP MPaa	H kJ/kg	SP MPaa	BPP	pH	Li	Na	K	Rb	Cs	Ca	Mg	Fe	Cl	F	SO_4	HCO_3	B	NH_3	SiO_2	H_2S	CO_2T
								mg/kg																
MG-1	6/1/81	Weber LP	1.198	1266	1.143	FBD	7.4	7.3	1974	354	1.96	0.85	15.1	0.09	0	3480	0	46	0	52	3.59	714	0	0
	10/7/94	Weber LP	2.99	1121	0.52	B6	7.15	6.8	1958	308	1.67	0.63	13	0.11	0.07	3363	1.36	30.3	83.9	44.7	3.14	720	2.93	76.57
MG-2D	11/14/81	Weber LP	1.212	1093	1.215	FBD	8	5.6	1880	333	1.84	0.57	22.5	0.06	0.05	3300	1.68	33	0	48.2	3.47	620	0	0
	10/14/82	Weber LP	2.598	1075	0.198	B4	8	7.1	2227	414	2.18	0.88	20.5	0.08	0.14	3767	1.89	38.1	0	57.5	2.38	755	0	0
MG-3D	9/16/92	Weber LP	1.43	2086	1.25	FBD	6.37	8.2	2391	578	2.95	0.65	71.8	0.26	0.6	4321	1.17	16.8	40.17	26.3	24.1	731	5.18	58.61
	12/2/92	Weber LP	5.794	1689	0.716	B4	7.29	10.5	3129	787	4.05	0.7	100	0.15	0.15	5750	1.26	10.8	31.74	37.8	24.1	852	1.86	25.6
MG-4D	11/26/90	Weber LP	0.116	812	0.095	FBD	8.21	3.2	1224	75	0.36	0.21	50.8	0.8	0.12	1692	0.36	303	0	20	1.25	283	0	0
MG-5D	8/19/83	Weber LP	0.628	1250	0.696	FBD	7.9	5.8	1675	271	1.35	0.52	21.4	0.3	0.95	3013	0.3	41	0	41.1	6.99	695	0	0
	10/17/83	Weber LP	2.195	1082	0.84	B2	8	4.9	1604	243	1.25	0.46	17.8	0.09	0.5	2703	0.43	70	0	34.6	5.96	671	0	0
MG-7D	1/10/91	Weber LP	3.03	1288	0.233	FBD	7.46	7.7	2108	421	2.43	0.78	24.5	0.04	0.12	3763	1.53	23.7	37.3	58.3	0	819	2.56	28.9
	6/13/93	Weber LP	3.245	1003	0.645	B3	6.62	7.3	2200	426	2.25	0.75	26.3	0.04	0.24	3792	1.08	21.5	34.19	55.4	2.46	760	4.4	47.13
MG-9D	4/26/94	Weber LP	1.874	1287	0.48	FBD	3.11	12	3117	950	3.68	0.85	81.7	25	282	6175	3.13	507.5	0	20.7	15.6	910	0.95	0
	3/11/95	Weber LP	3.443	1150	1.038	B3	3.31	12.1	3400	950	4.53	1.1	113	16.75	51.3	6428	1.79	68.4	0	19.5	14.1	923	3.07	0
MG-13D	10/31/94	Weber LP	0.965	1377	0.605	FBD	7.86	9.6	2567	550	3.40	1.08	7	0.13	0.14	4376	1.78	95.9	57.73	60.5	3.75	879	3.24	45.71
	10/29/94	Weber LP	4.12	1327	0.467	B5	7.66	9.9	2567	567	3.53	1.15	6	0.1	0.11	4568	1.77	69.3	39.02	62.3	4.51	911	2.9	30.88
MG-14D	8/16/94	Weber LP	0.733	1764	0.603	FBD	7.24	5.3	3233	700	3.68	0.9	21	0.32	0.2	5675	1.75	115.5	41.79	45.2	19.1	952	2.2	37.25
	8/8/94	Weber LP	3.793	1266	0.424	B4	7.44	4.5	3050	650	3.45	1.62	14	0.13	0.12	5417	1.54	29.1	58.63	42.4	17.6	915	2.56	47.53
MG-15D	12/17/94	Weber LP	0.952	1364	0.844	FBD	3.66	7.9	2507	600	2.93	0.84	53	10	24.3	4675	1.62	110.2	0	15.6	13.4	810	2.39	0
	12/15/94	Weber LP	2.542	1183	0.94	B2	3.44	0	2387	613	0.00	0	40	18	52.8	4352	2.2	161.8	0	15.5	6.64	851	3.2	0
MG-16D	9/296	Weber LP	0.865	1291	0.715	FBD	7.24	6.9	1919	554	3.90	1.58	31	0.01	0.1	3676	1.37	27.2	50.6	54	3.02	729	2.62	39.3
	9/22/94	Weber LP	2.65	1101	0.536	B2	7.26	7.8	2058	425	2.28	0.75	29	0.07	0.15	3631	1.27	24.4	44.96	52.3	2.13	719	3.34	39.14
MG-17D	11/23/94	Weber LP	0.672	1037	0.616	FBD	7.41	4.8	1453	180	0.70	0.37	17	0.22	0.06	2383	1.26	75.1	76.02	30.1	1.94	505	2.01	63.75
	12/8/94	Weber LP	1.012	1026	0.367	A2	7.75	4.9	1507	180	0.82	0.42	16	0.25	0.07	2551	1.31	80	73.94	32.2	1.9	531	2.04	58.55
MG-18D	1/17/95	Weber LP	0.91	1193	0.693	FBD	7.71	5.6	1854	283	1.65	0.75	5	0.06	0.06	2989	1.33	141	203.23	40.8	5.03	730	3.65	155.6
MG-19	1/2/95	Weber LP	1.223	1322	0.969	FBD	7.1	7.8	1942	400	2.25	1.51	16	0.09	0.12	3555	1.49	30.5	62.14	49.9	3.07	735	4.43	58.05
	1/12/95	Weber LP	2.853	1238	1.231	B2	7.06	7.9	1975	375	1.95	0.75	16	0.1	0.09	3420	1.5	25.2	63.96	47.6	3.41	708	3.14	57.42
MG-20D	1/24/96	Weber LP	0.602	1131	0.56	FBD	3.3	6.1	2183	450	1.95	0.5	45	16.1	50	4120	1.4	307	0	16.2	7.98	626	1.87	0
	1/27/96	Weber LP	1.332	1037	0.39	A1	2.98	6.6	2317	483	1.98	0.5	27	15.9	59	4212	1.7	329.2	0	15.8	7.92	665	1.36	0
MG-21D	10/17/95	Weber LP	0.552	1581	0.47	FBD	3.57	8.3	2950	600	2.33	0.74	50	25	131	5418	3.15	556	0	25.7	12	795	4.26	0
	10/9/95	Weber LP	0.742	1181	0.64	A5	3.29	6.5	2492	467	1.70	0.64	20	15.53	58.5	4322	2.88	358	0	20.7	9.08	696	0.68	0
MG-22D	8/12/96	Weber LP	0.675	1290	0.325	FBD	7.64	6.4	2029	400	3.57	0.91	35	0.16	0.12	3421	1.5	32.3	49.3	48.2	2.14	709	2.4	36.9
	9/16/96	Weber LP	2.52	1217	0.515	B2	7.57	7.3	1849	357	2.20	0.65	26	0.06	0.25	3479	1.48	31	53.3	49	2	707	2.9	40.1
MG-23D	6/24/96	Weber LP	1.268	1334	0.693	FBD	7.32	6.7	1861	350	1.90	0.7	17	0.08	0	3304	1.03	29.7	65.3	48.2	2.7	710	2.22	51
	7/22/96	Weber LP	2.443	1160	0.543	B1	7.07	6.3	1709	333	2.40	0.9	21	0.1	0.01	3294	1	30.5	73	45.2	3.23	744	2.56	61
MG-24D	7/19/96	Weber LP	1.142	1856	0.368	FBD	6.74	6.7	2165	400	3.03	1.02	29	0.2	0.2	4073	1.7	108.5	199	26.2	11.7	893	2.73	180
	2/17/97	Weber LP	2.667	1624	0.906	B2	6.95	7	2226	551	2.74	0.72	50	1.23	0.7	4123	1.42	64.1	159.3	27	5.45	813	0	133.5

Table 2 : Representative Gas Discharge Chemistry

Well Name	Date	Source	WHP MPaa	H kJ/kg	SP MPaa	BPP	CO_2	H_2S	NH_3	Residual Gas	He	H_2	Ar	N_2	CH_4	Cl mg/kg
							mmoles/100 moles									
MG-1	6/1/81	Weber Low Pressure	1.198	1266	1.129	FBD	942	6.93	0	0	0	0	0	0	0	0
	10/7/94	Weber Low Pressure	2.99	1121	0.52	B6	1007	12.29	2.12	3.092	0	0.034	0	0	0.58	10
MG-2D	11/14/81	Weber Low Pressure	1.212	1093	1.21	FBD	682	6.7	1.67	12.3	0	0	0	0	0	11
	10/14/82	Weber Low Pressure	2.598	1075	0.212	B4	293.8	4.23	1.43	2.23	0	0.046	0	1.452	0.053	36
MG-3D	9/16/92	Weber Low Pressure	1.43	2086	1.25	FBD	1758	38.3	6.29	0	0	2.09	0	8.44	0.93	13
	12/2/92	Weber Low Pressure	5.794	1689	0.716	B4	1312	28.2	6.57	0	0	39.05	0	127.3	12.7	107
MG-4D	11/26/90	Weber Low Pressure	0.116	812	0.115	FBD	684	3.17	1.6	32.38	0	0.572	0	28.07	3.41	42
MG-5D	8/19/83	Weber Low Pressure	0.628	1250	0.558	FBD	6495	15.4	3.43	51.78	0	1.757	0	20.88	23.1	14
	10/17/83	Weber Low Pressure	2.195	1082	0.84	B2	5771	16.9	3.51	0	0	0	0	0	0	4
MG-7D	1/10/91	Weber Low Pressure	3.03	1288	0.233	FBD	504	9.22	1.26	3.935	0	0.343	0	3.024	2.49	0
	6/13/93	Weber Low Pressure	3.245	1003	0.645	B3	798	17.8	1.6	4.603	0	0.174	0.1	5.355	0.81	0
MG-9D	4/26/94	Weber Low Pressure	1.874	1287	0.48	FBD	400	24.3	0.05	16.835	0	0.082	0.1	12.67	0.65	0
	3/11/95	Weber Low Pressure	3.443	1150	1.038	B3	538	31.2	0.07	4.707	0	1.272	0	2.75	0.68	0
MG-13D	10/31/94	Weber Low Pressure	0.965	1377	0.605	FBD	592	18.77	2.8	3.314	0	0.112	0	0.914	0.871	9
	10/29/94	Weber Low Pressure	4.12	1327	0.467	B5	587	17.7	2.71	4.539	0	0.205	0	0.056	1.24	7.6
MG-14D	8/16/94	Weber Low Pressure	0.733	1764	0.603	FBD	1436	22.4	7.69	4.303	0	2.11	0	0.36	1.73	114
	8/8/94	Weber Low Pressure	3.793	1266	0.424	B4	1417	19.3	8	7.272	0.1	0.167	0	4.273	0.43	14
MG-15D	12/17/94	Weber Low Pressure	0.952	1364	0.844	FBD	833	32.2	0.16	12.261	0	1.174	0	6.651	4.05	27
	12/15/94	WeberLow Pressure	2.542	1183	0.94	B2	929	51.1	0.05	8.795	0.	2.162	0	4.038	3.3	7
MG-16D	9/2/96	Weber Low Pressure	0.865	1291	0.715	FBD	482	9.39	1.33	4.145	0	0.207	0.045	3.459	0.433	0
	9/22/94	Weber Low Pressure	2.65	1101	0.536	B2	505	5.29	0.98	6.08	0	0.054	0	0	0.19	13
MG-17D	11/23/94	Weber Low Pressure	0.672	1037	0.616	FBD	741	9.6	1.4	6.854	0	0.051	0	4.253	1.79	22
	12/8/94	Weber Low Pressure	1.012	1026	0.367	A2	602	8.45	1.56	3.783	0	0.036	0	1.848	1.07	0
MG-18D	1/17/95	Weber Low Pressure	0.913	1193	0.693	FBD	1239	12.2	2.42	5.471	0	0.115	0	2.117	1.61	16
MG-19	1/2/95	Weber Low Pressure	1.223	1322	0.969	FBD	771	15.7	4.16	4.823	0	0.118	0	3.158	1.31	136
	1/12/95	Weber Low Pressure	2.853	1238	1.231	B2	919	17.3	1.81	5.648	0	0.17	0	2.985	1.69	32
MG-20D	1/24/96	Weber Low Pressure	0.602	1131	0.562	FBD	921	46.6	0.08	33.851	0.001	5.859	0.337	22.558	5.094	5
	1/27/96	Weber Low Pressure	1.332	1037	0.392	A1	793	41	0.02	30.071	0.002	8.528	0.275	16.811	4.455	11
MG-21D	10/17/95	Weber Low Pressure	0.552	1581	0.47	FBD	716	92.2	0.24	58.705	0	4.07	0.697	51.578	2.36	25
	10/9/95	Weber Low Pressure	0.742	1181	0.64	A5	1031	148	0.24	38.758	0	5.755	0.462	29.326	3.215	20
MG-22D	8/12/96	Weber Low Pressure	0.675	1290	0.33	FBD	407	11.93	1.38	3.545	0.002	0.13	0.055	2.462	0.897	48
	9/16/96	Weber Low Pressure	2.52	1217	0.52	B2	537	7.99	1.56	3.513	0.001	0.147	0.036	2.518	0.812	41
MG-23D	6/24/96	Weber Low Pressure	1.268	1334	0.693	FBD	638	10.95	2.23	6.852	0	1.092	0.067	4.291	1.132	24
	7/22/96	Weber Low Pressure	2.443	1160	0.543	B1	802	9.36	1.76	7.251	0	0.2	0.086	5.643	1.823	0
MG-24D	7/19/96	Weber Low Pressure	1.142	1856	0.368	FBD	3361	17.9	4.37	4.669	0.011	3.102	0.02	2.246	38.858	23
	2/17/96	Weber Low Pressure	2.667	1624	0.906	B2	3816	27.5	6.31	26.317	0.002	2.085	0.061	7.334	16.835	6